AV Integrated Reservoir Modeling of the Natih E Member at a Salt-cored Carbonate Dome, Jebel Madar, Oman*

Johan S. Claringbould[1,2], J Frederick Sarg[1], Brittney B. Hyden[1], and Bruce D. Trudgill[1]

Search and Discovery Article #110161 (2011)
Posted June 20, 2011

*Adapted from oral presentation at Session: Seismic Reservoir Characterization, at AAPG Annual Convention and Exhibition, Houston, Texas, USA, April 10-13, 2011

[1]Geology and Geological Engineering, Colorado School of Mines, Golden, CO
[2]Currently Columbia University, New York, NY (claringbould@ldeo.columbia.edu)

Abstract

The Upper Cretaceous fractured carbonates of the Middle East contain some of the world's largest hydrocarbon reserves. Besides matrix permeability and porosity, reservoir quality is highly dependent on fracture distribution. The northern Oman region has a complex tectonic history, and multiple major tectonic events affected the area.

This study provides a three-dimensional structural evolution of the Upper Cretaceous outcrops of a salt-cored domed structure containing reactivated faults (Jebel Madar) that crop out in the Adam Foothills of Northern Oman. A multi-layered, integrated, three-dimensional, numerical structural model of the study area was built to determine the impact of multiple major tectonic events to the fault and fracture distribution in the study area. Data types and scales include: geologic field mapping, photo-realistic LiDAR models, high-resolution Quickbird imagery, depth elevation models, and seismic and well-log data.

Analysis of the structural evolution of Jebel Madar shows that three major tectonic events with different stress regimes resulted in a complex domed structure containing reactivated faults. NE-SW-oriented graben- and half-graben structures formed as a result of initial local dome-formation, due to SW-verging compression of the Late Cretaceous obduction of the Hawasina Complex and Semail Nappe to the NNE of the study area. Seismic interpretation shows that the imbricates of the allochthonous Hawasina Complex were deposited across the study area, causing burial of approximately 1 km and resulting in initial fluid release and calcite formation as fault infill. Early Paleocene obduction of the Masirah ophiolite, east of the study area and the opening of the Gulf of Aden, led to a NW-verging transtensional stress regime that caused E-W-oriented oblique normal fault formation, cross-cutting pre-existing faults in the study area. Lastly, the Miocene Alpine orogeny resulted in growth of the Oman Mountains north of the study area and a foreland basin formation in the Adams Foothills, which led to local dome-formation by reactivation of the pre-existing faults and salt diapirism as a result of differential loading. This event is marked by clear down-dip slickenlines on the fault surfaces, fault breccia containing a mix of calcite and blocks of older stratigraphy, and locally reactivated folding.

Selected References

Glennie, K.W., 1995, The Geology of the Oman Mountains: an outline of their origin: Scientific Press, Beaconsfield, 92 p.

Lønøy, A., 2006, Making sense of carbonate pore systems: AAPG Bulletin, v. 90/9, p. 1381-1405.

Peters, J.M., J.B. Filbrandt, J.P. Grotzinger, M.J. Newall, M.W. Shuster, and H.A. Al-Siyabi, 2003, Surface-piercing salt domes of interior North Oman, and their significance for the Ara carbonate "stringer" hydrocarbon play: GeoArabia Manama, v. 8/2, p. 231-270.

Pollastro, R.M., 1999, USGS OpenFile Report #OF99-0050-D, *in* R.M. Pollastro, (ed.) Ghaba salt basin province and Fahud salt basin province, Oman; geological overview and total petroleum systems.

Van Buchem, F.S.P., P. Razin, P.W. Homewood, J.M. Philip, G.P. Eberli, J-P. Platel, J. Roger, R. Eschard, G.M.J. Desaubliaux, T. Boisseau, J-P. Leduc, R. Labourdette, and S. Cataloube, 1996, High resolution sequence stratigraphy of the Natih Formation (Cenomanian/Turonian) in northern Oman; distribution of source rocks and reservoir facies: GeoArabia Manama, v. 1/1, p. 65-91.

Integrated Reservoir Modeling of the Natih E Member at a Salt-cored Carbonate Dome, Jebel Madar, Oman

Johan S. Claringbould*, J. Frederick Sarg, Brittney B. Hyden, Terrance R. Birdsall

Colorado School of Mines, Department of Geology and Geological Engineering, 1516 Illinois Street, Golden, Colorado, USA

Jean-Christophe Embry, Giulio Casini, Stephane Homke, John B. Thurmond, David W. Hunt

Statoil ASA, Research Centre, Sandsliveien 90, Bergen, P.O. Box 7200, N-5020, Bergen, Norway

*present address: Lamont-Doherty Earth Observatory of Columbia University, 61 Route 9W, Palisades, New York, USA,

contact: claringbould@ldeo.columbia.edu

COLORADO SCHOOL OF MINES
EARTH • ENERGY • ENVIRONMENT

Statoil

Acknowledgements

- Statoil Research Centre in Bergen
- Colorado School of Mines – Dept. Geology and Geological Engineering
- Université Bordeaux 3: Carine Grélaud
- AAPG

Objectives

- Analogue reservoir model – calibrated to field
- Build three-dimensional integrated multi-layered reservoir model – generate workflow

- Fracture distribution analyses – 5 photo-realistic LiDAR Models and 21 fracture maps
- Lithofacies, porosity, permeability distribution analyses – 9 stratigraphic sections and SEM QEMSCAN® analyses of 200 samples
- Integrated geomodel – stratigraphic and structural field data, high resolution Quickbird imagery, and 30-meter ASTER DEM

Study Area

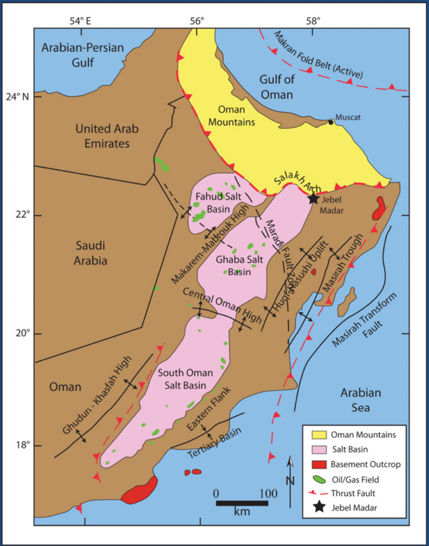

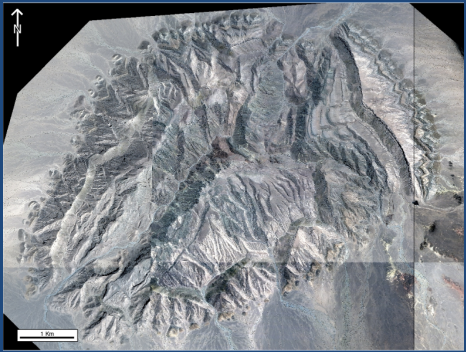

Modified after Pollastro (1999) and Peters *et al.* (2003)

Presenter's notes: Dome dimensions--7 km across, 750 m high.

Regional Geology - Stratigraphy

Chronostratigraphy: Age (Ma)	Era	Period	Epoch	Autochthonous Rock Units: Supergroup	Group	Formation
0-1.6	Cenozoic	Q	Recent Pleist.		Fars	Fars
5		Tertiary	Pliocene			
23			Miocene			
35			Oligocene			
56			Eocene		Hadhramaut	Dammam/Rus
65			Paleocene			Umm er Radhuma
74	Mesozoic	Cretaceous	Masstrichtian		Aruma	Simsima
83			Campanian			Muti (Fiqa)
			Santonian			
			Coniacian			
93			Turonian		---- gap ----	
97			Cenomanian	Hajar Supergroup	Wasia	Natih
112			Albian			Nahr Umr
			Lower		Kahmah	Shuaiba Kharaib Lekhwair Habshan/Salil/Rayda
145		Jurassic	Upper		Sahtan	Jubaila/Hanifa
157			Middle			Tuwaiq Dhruma
178			Lower			Mafraq
205		Triassic	Upper		Akhdar	Mahil
251			Lower			Jilh Sudair
270	Paleozoic	Permian	Upper			Khuff
290			Lower		Haushi	Gharif Rahab Al Khlata

Modified after Glennie (1995)

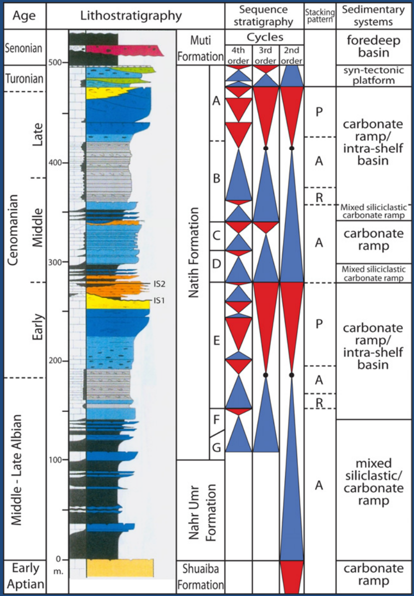

Modified after Razin *et al.* (2007)

Presenter's notes: Late Cretaceous obduction; Miocene Alpine orogeny.

Jebel Madar

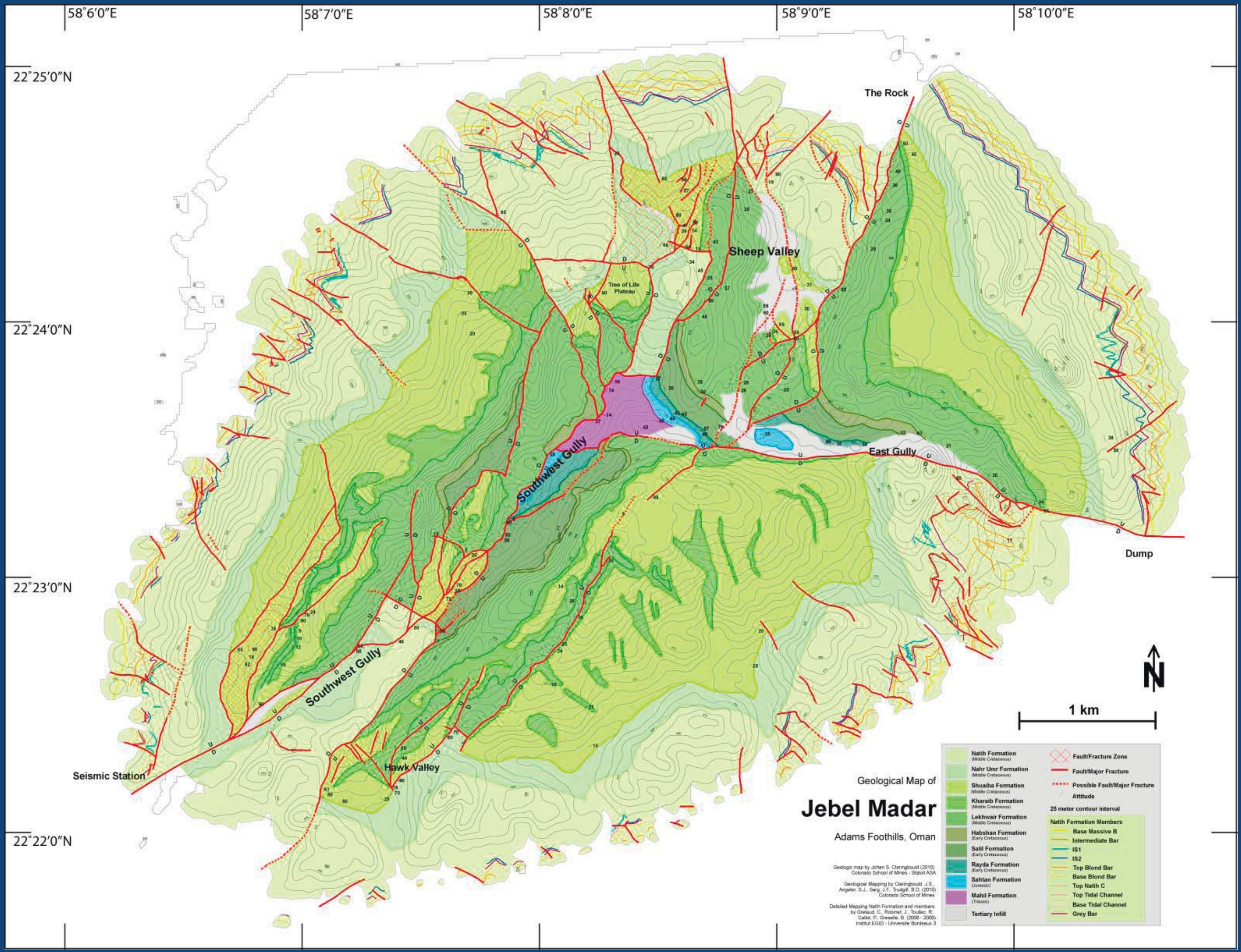
58°6'0"E
58°7'0"E
58°8'0"E
58°9'0"E
58°10'0"E
22°25'0"N
22°24'0"N
22°23'0"N
22°22'0"N
The Rock
Sheep Valley
Tree of Life Plateau
East Gully
Southwest Gully
Southwest Gully
Dump
Hawk Valley
Seismic Station
1 km
N
Geological Map of
Jebel Madar
Adams Foothills, Oman
Geologic map by Johan S. Claringbould (2010)
Colorado School of Mines - Statoil ASA
Geological Mapping by Claringbould, J.S., Angeter, S.J., Sarg, J.F., Trudgill, B.D. (2010)
Colorado School of Mines
Detailed Mapping Natih Formation and members by Grelaud, C., Robinet, J., Toullec, R., Callot, P., Gresselle, B. (2008 - 2009)
Institut EGID - Universite Bordeaux 3
Natih Formation (Middle Cretaceous)
Nahr Umr Formation (Middle Cretaceous)
Shuaiba Formation (Middle Cretaceous)
Kharaib Formation (Middle Cretaceous)
Lekhwair Formation (Middle Cretaceous)
Habshan Formation (Early Cretaceous)
Salil Formation (Early Cretaceous)
Rayda Formation (Early Cretaceous)
Sahtan Formation (Jurassic)
Mahil Formation (Triassic)
Tertiary Infill
Fault/Fracture Zone
Fault/Major Fracture
Possible Fault/Major Fracture
Attitude
25 meter contour interval
Natih Formation Members
Base Massive B
Intermediate Bar
IS1
IS2
Top Blond Bar
Base Blond Bar
Top Natih C
Top Tidal Channel
Base Tidal Channel
Grey Bar

Introduction | **Data and Processing** | Modelling | Discussion | Conclusions

Data and Processing

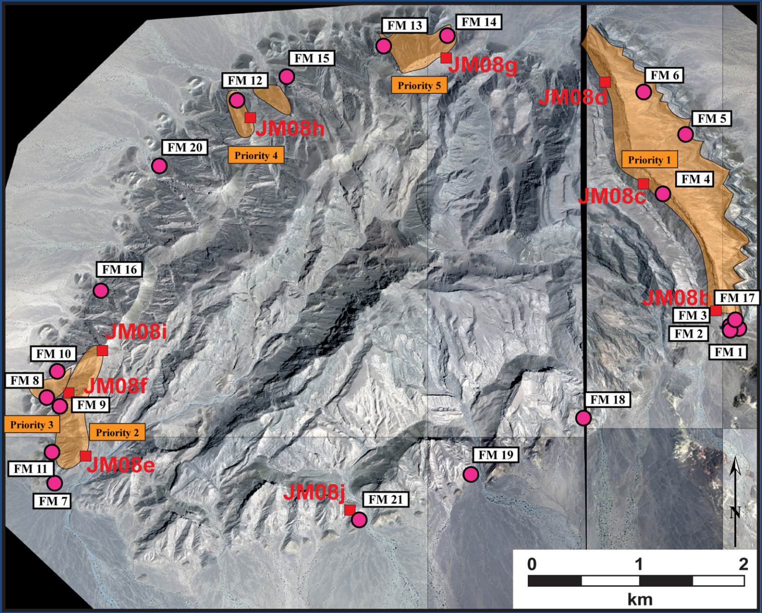

Presenter's notes: Quickbird imagery and ASTER DEM model; geo- and ortho-rectified combined Quickbird images; 30-meter ASTER DEM.

Lithofacies distribution

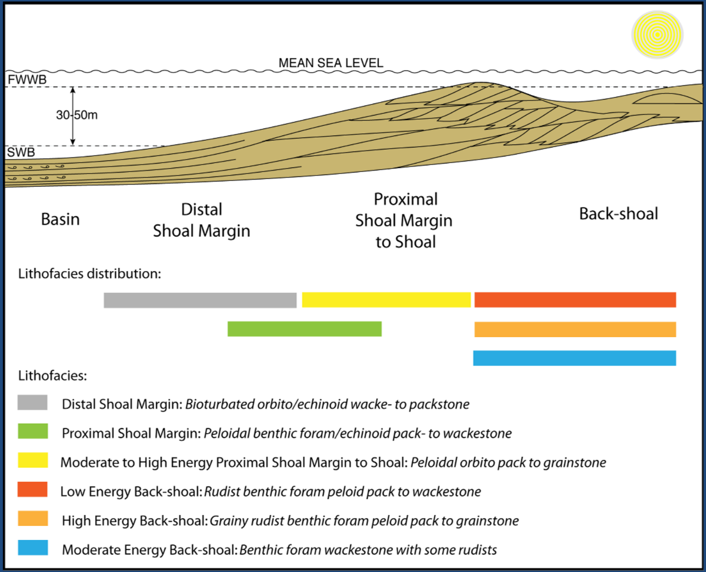

Modified after van Buchem *et al.* (1996)

Presenter's notes: Six lithofacies in three facies associations in Natih E Member; Mid-ramp position, patchy inactive to active back-shoal.

Lithofacies Correlation

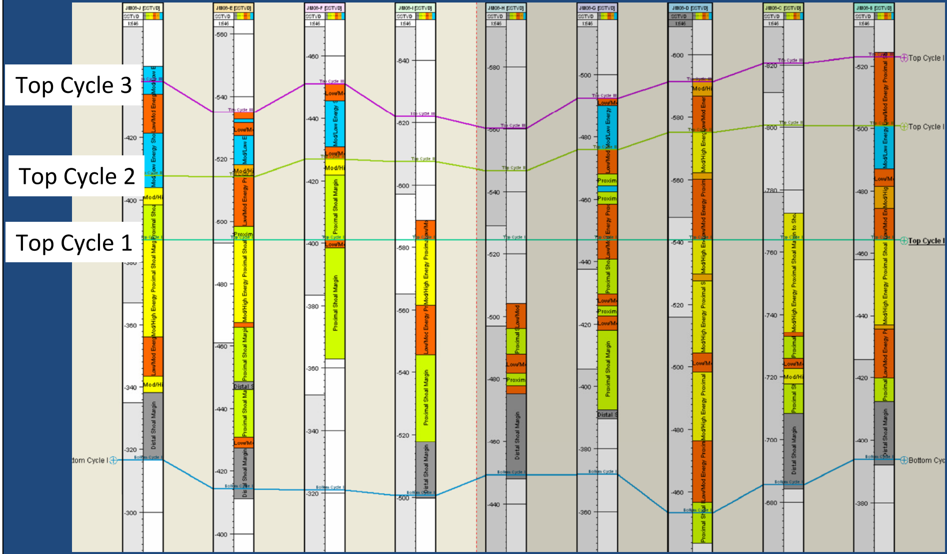

Presenter's notes: Three depositional cycle tops correlated in Natih E Member, aggrading shoaling upward fourth order cycles.

Porosity and Permeability

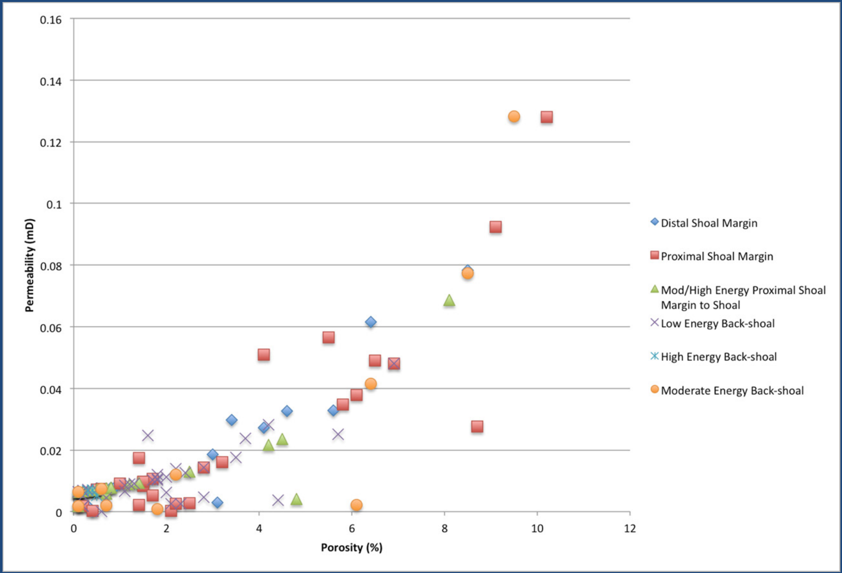

Presenter's notes: QEMSCAN analyses of 200 samples, Lønøy (2006) classification scheme.

Porosity and Permeability

- Dominant micro-rhombic low-Mg lime mud, interconnected mudstone microporosity
- Grainstones: moldic microporosity

- Low average porosity (0.3 – 4.8 %)
- Low average permeability (0.002 – 0.028 mD)

Fracture Distribution – Field

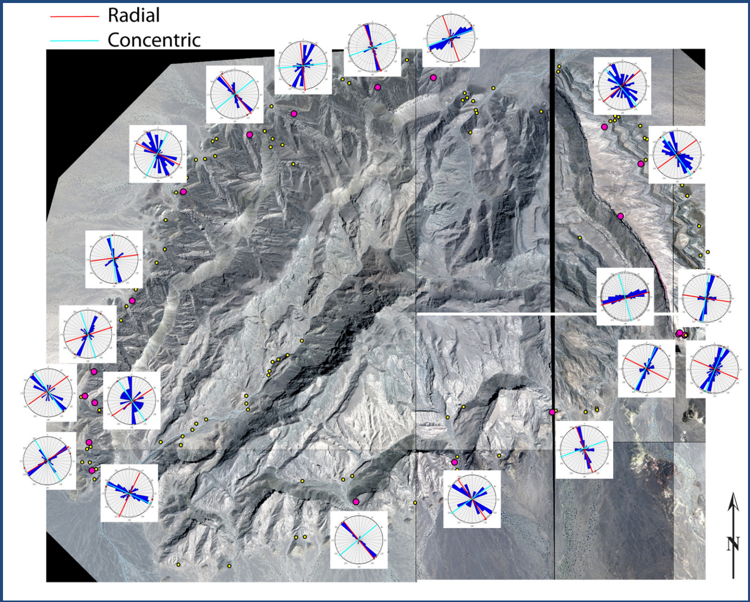

Presenter's notes: 8x8 m fracture maps--radial and concentric fractures superimposing earlier fracture sets.

Fracture Distribution – Field

- Fracture Maps:
  - Primary trend: NNW – SSE and NNE – SSW
  - Secondary trend: NW – SE and ENE – WSW
  - Dominant concentric and radial fractures(superimposed to reactivated)
  - High angle dip (~80 – 90 degrees)
  - Fracture swarms near major faults

Introduction | Data and Processing | Modelling | Discussion | Conclusions

Fracture Distribution - LiDAR

- Photo-realistic LiDAR
  - Concentric fractures (av. FH: 14.3 m, av. FD: 0.09 frac/m)
  - Radial fractures (av. FH: 23 m, av. FD: 0.08 frac/m)
  - No consistent fracture swarm distribution

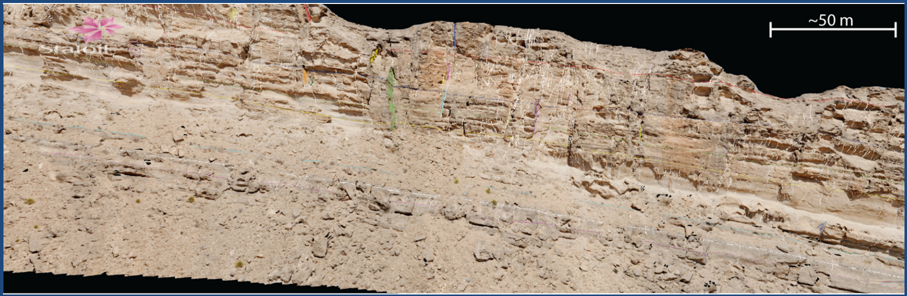

Presenter's notes: Dominant radial and concentric fractures; high-angle dips (~75 – 90 degrees).

Integrated Geomodeling

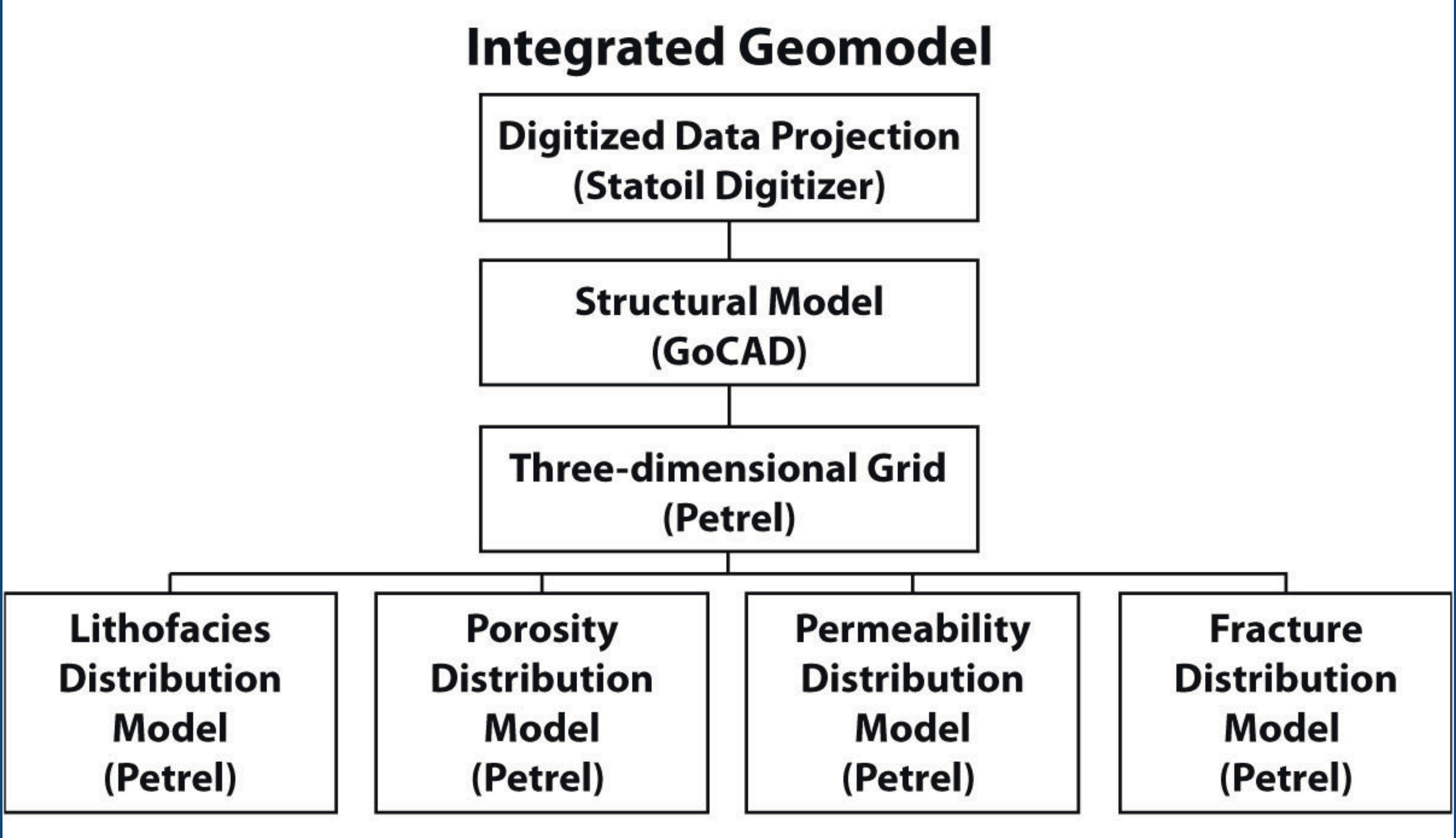

Digitized Data Projection

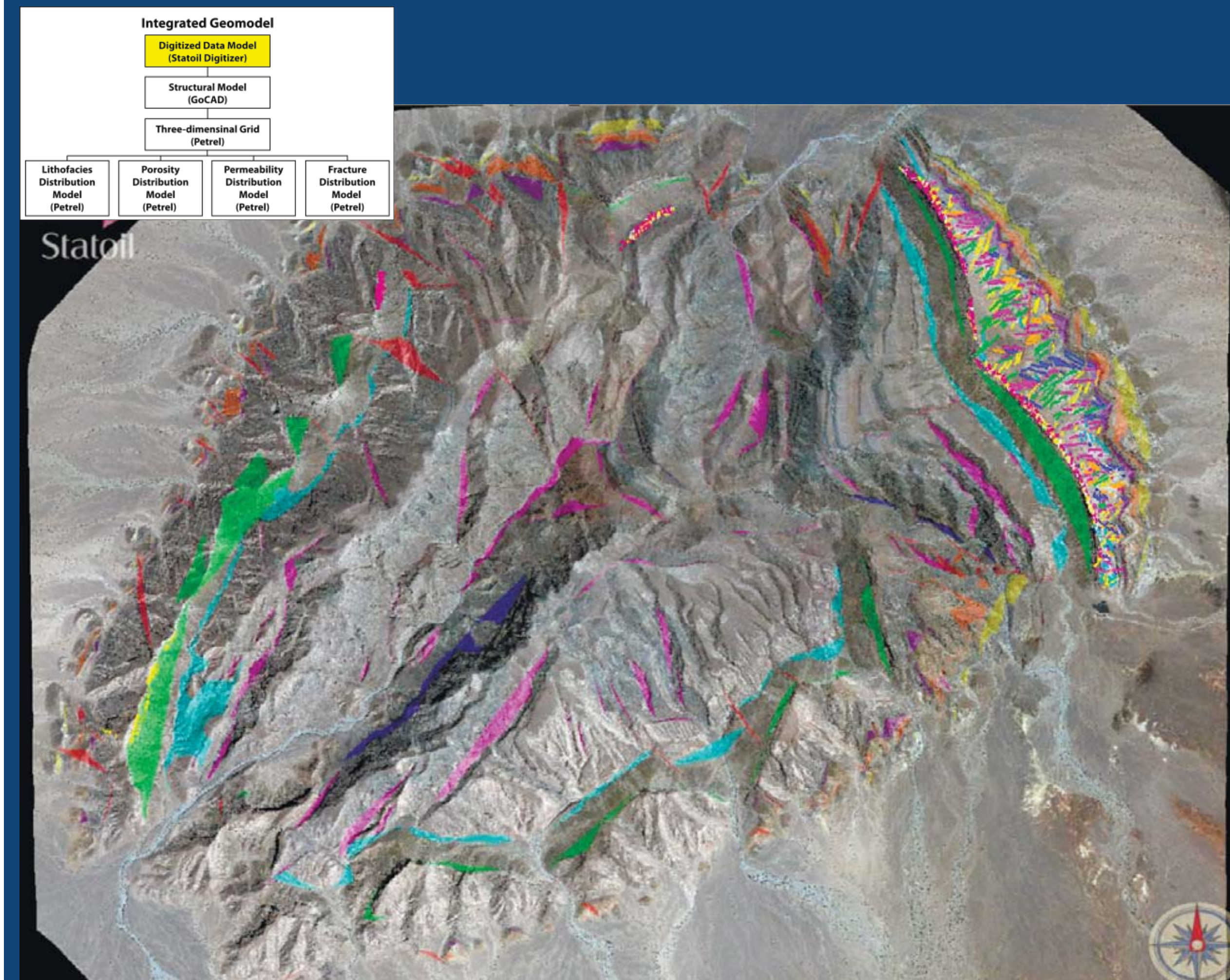

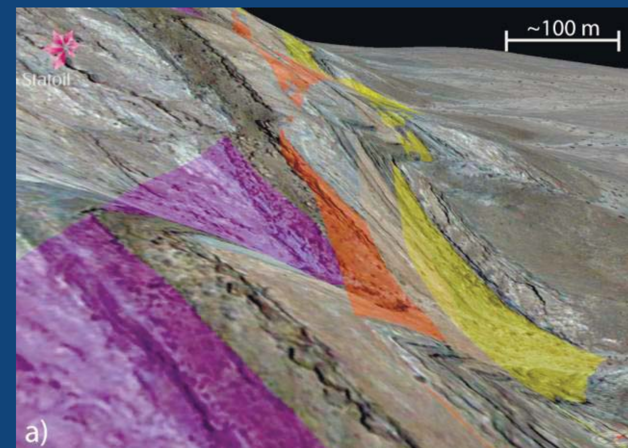

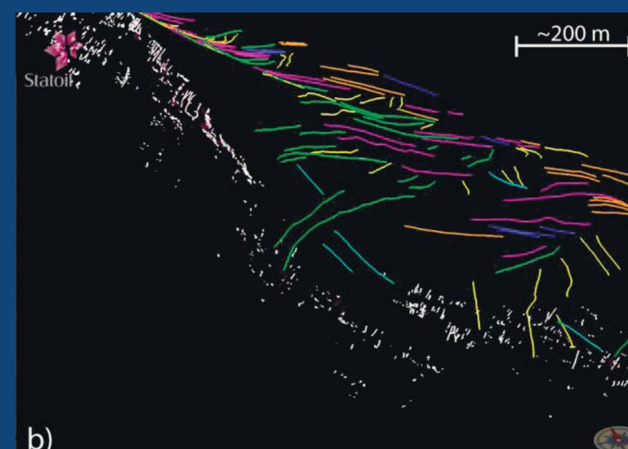

Structural Model

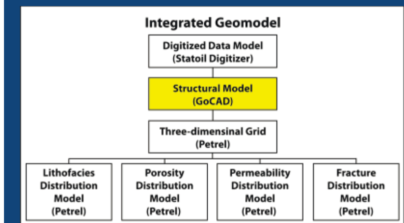

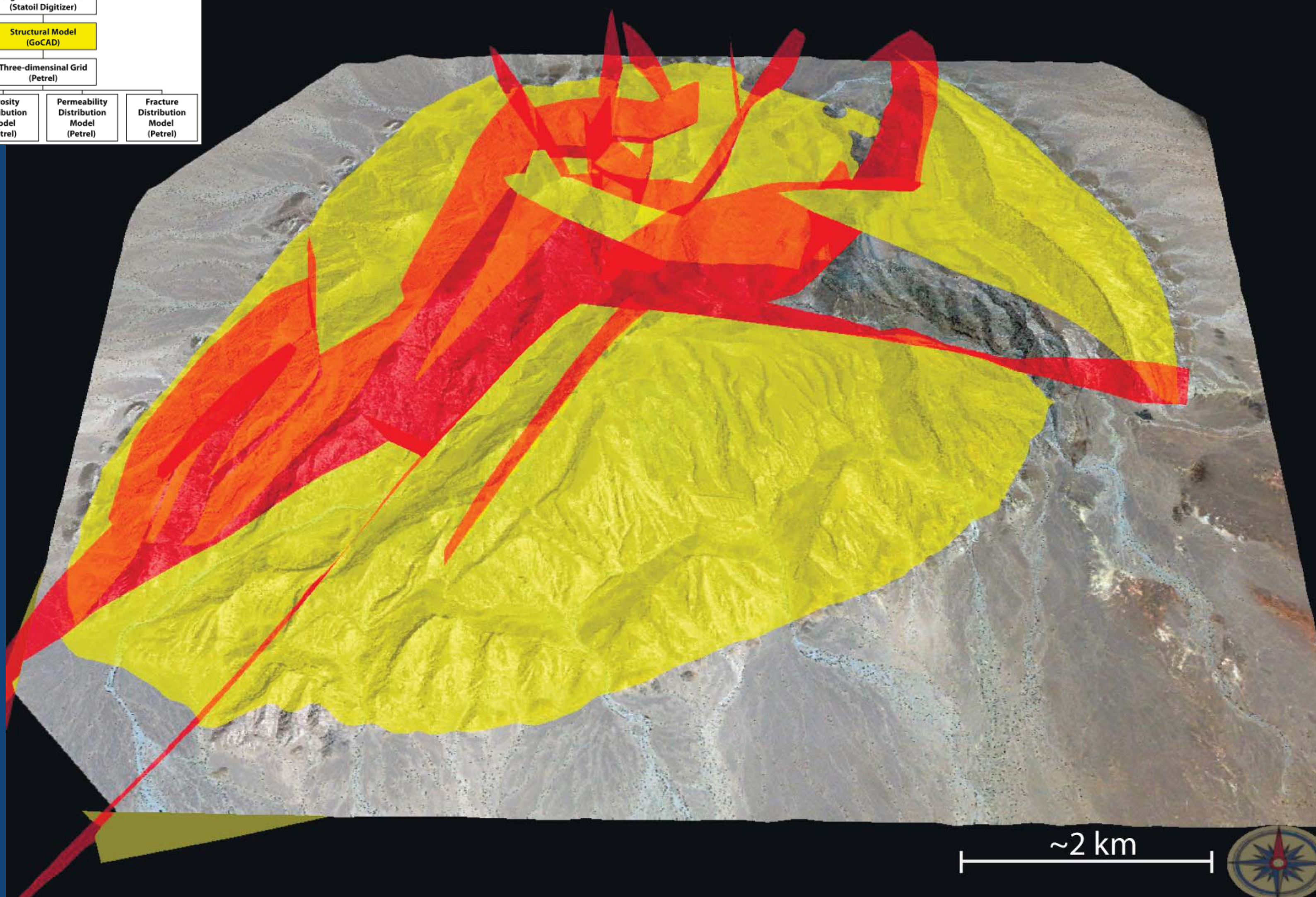

Introduction | Data and Processing | **Modeling** | Discussion | Conclusions

Structural Model

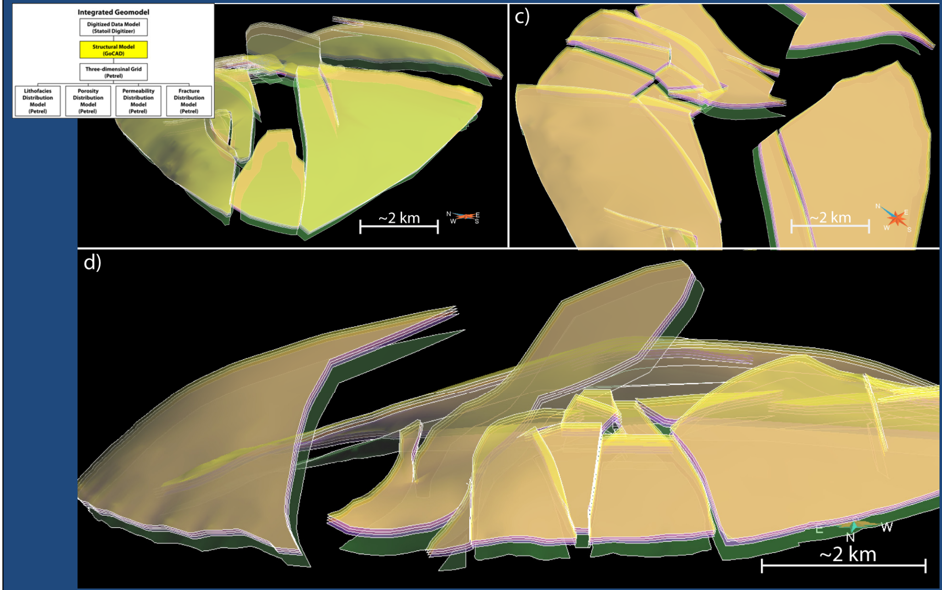

Presenter's notes: Curvature/dips based on field measurements.

Three-dimensional Grid

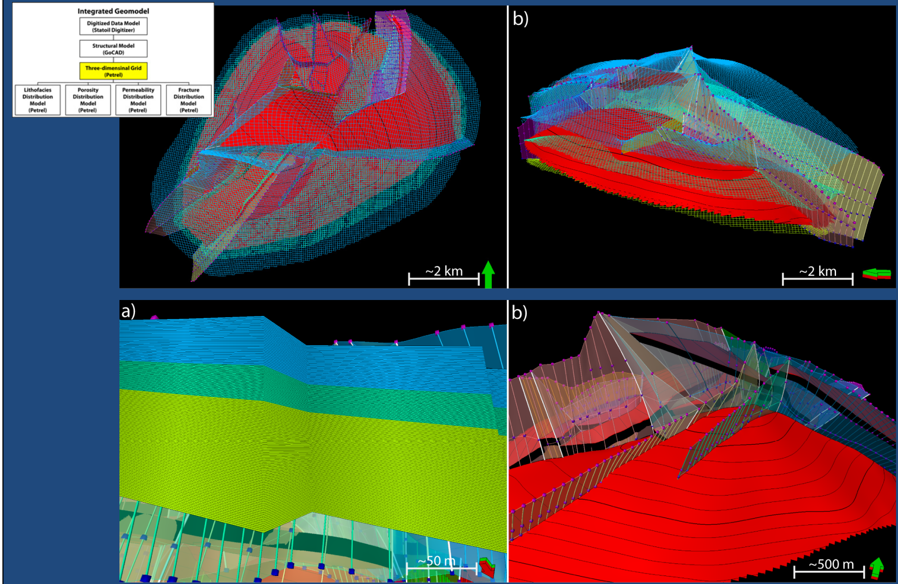

Presenter's notes: 50 x 50 meter cells – over 3 million cells.

Click to view notes for the slide.

Lithofacies Distribution Model

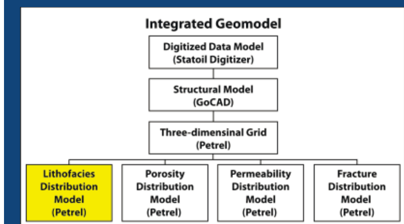

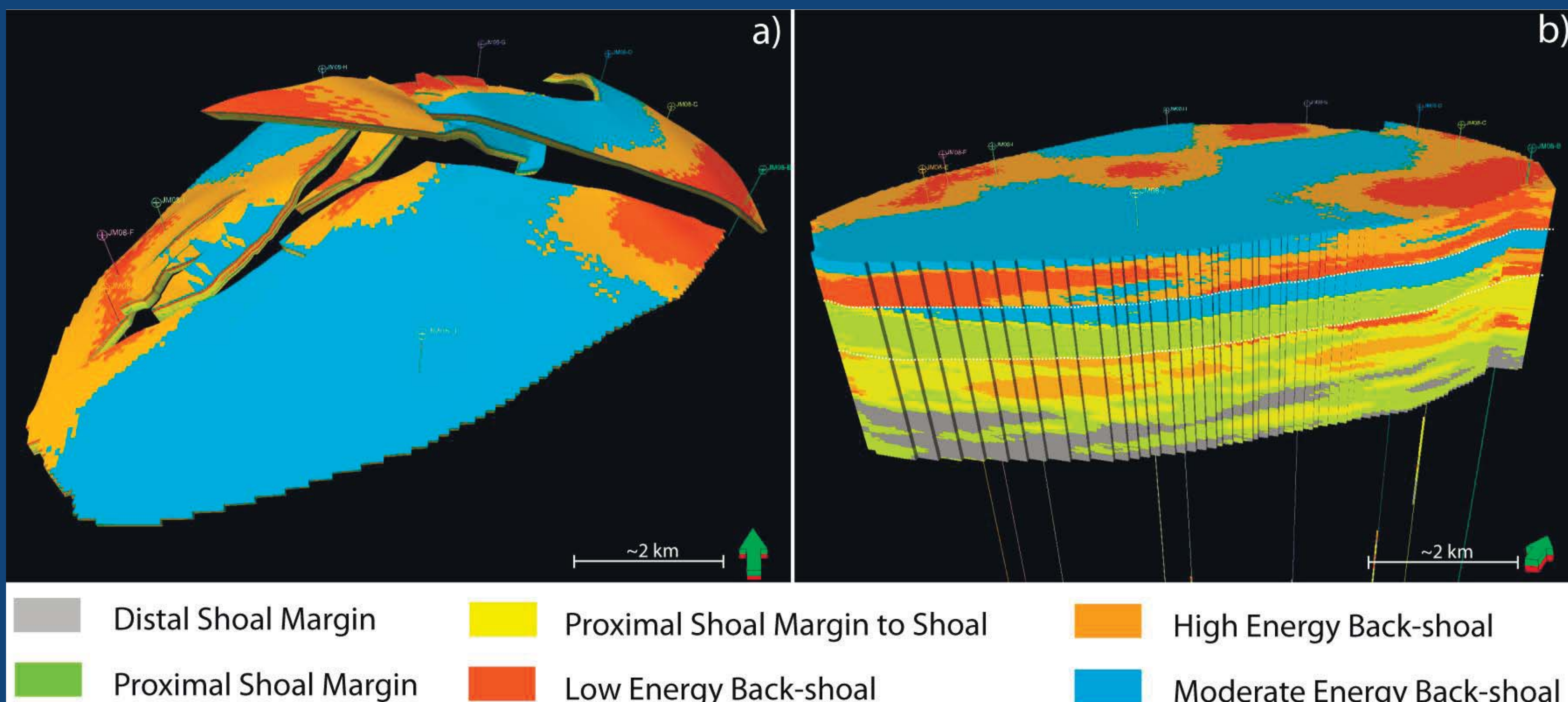

Presenter's notes: Sections used as pseudo-wells. Combination of two different distribution algorithms (Trial and Error): "Truncated Gaussian Simulation with trends" and "Object Modelling" algorithms.
Ellipsoidal form of 1000 m in the major direction, 1000 m in the minor direction, 8 m in the vertical direction, a dip of 0 degrees, and a vertical variance of 0.8.
The vertical geometry of the distribution had a trend with an azimuth of 218, with a line source and progradational distribution.
Distal lithofacies – trending 218 and always bound in order. Back-shoal lithofacies – trending 218, not bound in order; are more patchy.
Trial and error--calibrated to field data.

Lithofacies Distribution Model

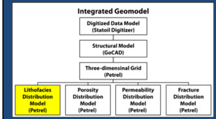

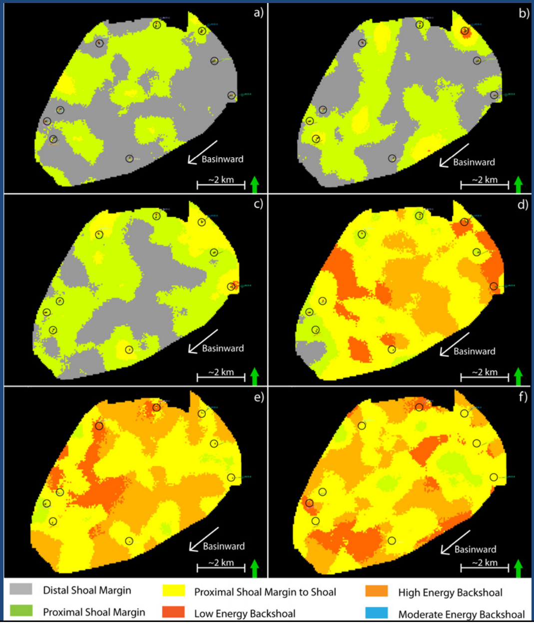

Presenter's notes: Results based on field observations, not on algorithm.

Porosity Distribution Model

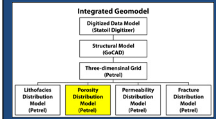

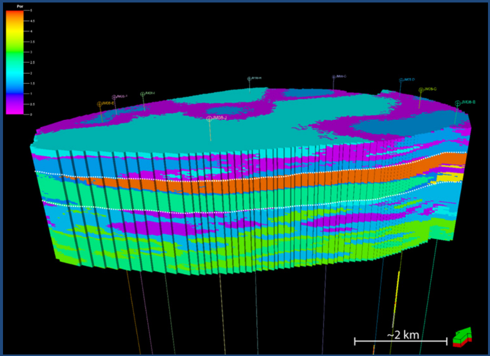

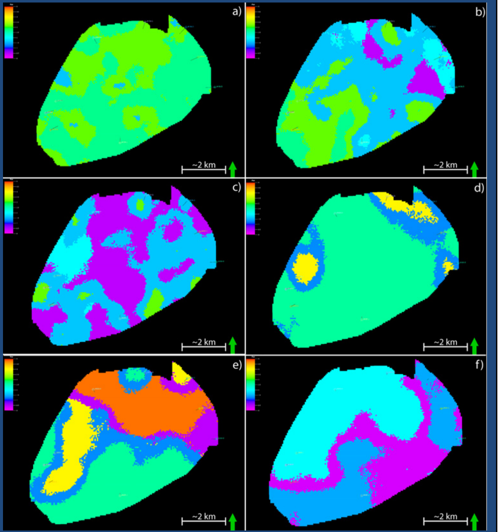

Presenter's notes: Based on lithofacies distribution. Variable but low average porosity (0-5%). No clear distribution trend. Not dependent on lithofacies or sample location. Reservoir quality of Natih E Member is highly dependent on fracture network.

Permeability Distribution Model

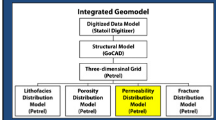

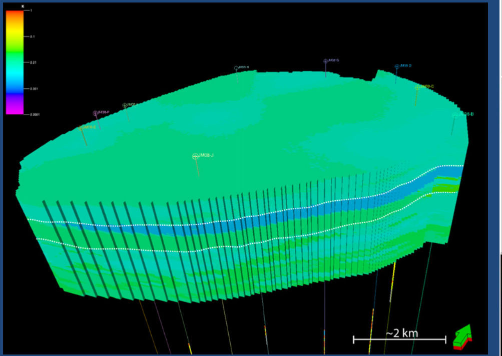

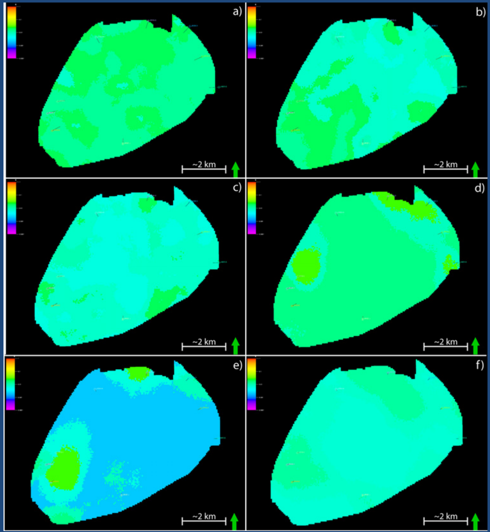

Presenter's notes: 0.001 mD – 1mD (around 0.01mD).

Fracture Distribution Model

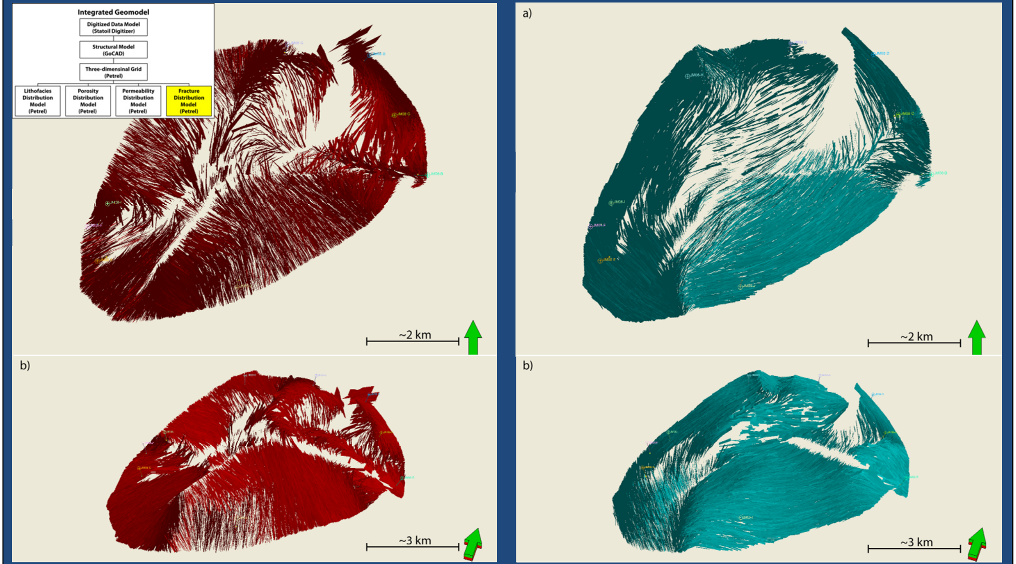

Presenter's notes: No clear fracture distribution within lithofacies or location. Orientation all around, but abundant radial and concentric. Fractures heights – variable. Fracture density – consistent. Distribution – through whole grid: no density of preferred orientation change. Concentric/Radial fractures considered to have biggest impact on reservoir quality as they are larger (vertically and laterally). They are more likely to be open or partially cemented than regional ones.

Integrated Geomodeling

- Limitations:
  - Quality of field area and resolution of data models
  - Quality and quantity of data in field and models
  - Limitations of workflow and software

- However, since richness and quality of the data are high, biases are minimized.

Conclusions

- Stratigraphic framework of Natih E Member: three shoaling-upward fourth-order depositional cycles, six lithofacies
- Facies occupy mid-ramp position: quiet subtidal shelf environment with inactive to active shoal
- Porosity and permeability: low, no clear distribution
- Dominant fracture orientations: concentric and radial – superimposed to reactivated

Presenter's notes: Field data--Shoaling upward, within framework of SW- basinward direction.

Conclusions

- Integrated geomodel
  - Component models: structural, 3D grid, lithofacies, porosity, permeability, and fracture
  - Based on different data types and scales
  - Calibrated to the field
  - Workflow is simple, but with limitations

Presenter's notes: "All models are wrong; some of them are useful."